MINISTRY OF EDUCATION AND TRAINING
VIETNAM ACADEMY OF SCIENCE AND TECHNOLOGY

GRADUATE UNIVERSITY OF SCIENCE AND TECHNOLOGY

DINH THI TU

ISOLATION, PURIFICATION OF CURCUMIN AND SEMI-SYNTHESIS OF ITS DERIVATIVES GUIDED BY *in vitro* AND *in silico* BIOLOGICAL ACTIVITIES FROM VIETNAMESE TURMERIC (*Curcuma longa* L.)

DISSERTATION ABSTRACT MATERIALS SCIENCE

Natural Products Chemistry Code: 9.44.01.17

HA NOI – 2026

The dissertation is completed at: Graduate University of Science and Technology, Vietnam Academy Science and Technology

Supervisors:

1. Supervisor 1: Associate Professor, Dr. Pham Minh Quan
   Institute of Chemistry - Vietnam Academy of Science and Technology
2. Supervisor 2: Associate Professor, Dr. Ngo Kim Chi
   Institute of Chemistry - Vietnam Academy of Science and Technology

Referee 1: Associate Professor, Dr. Nguyen Thi Hong Van, Institute of Chemistry - Vietnam Academy of Science and Technology

Referee 2: Associate Professor, Dr. Pham Thi Tam, Hanoi Open University

The dissertation will be examined by Examination Board of Graduate University of Science and Technology, Vietnam Academy of Science and Technology at …….

The dissertation can be found at:

1. Graduate University of Science and Technology Library
2. National Library of Vietnam

LIST OF THE PUBLICATIONS RELATED TO THE DISSERTATION

1. **Tu Thi Dinh**, Quan Minh Pham, Long Quoc Pham, Chi Kim Ngo, Van Thi Thuy Nguyen, Thuong Thi Le Hoang, Tu Ngoc Ly, Linh Ngoc Nguyen, Thao Thi Phuong Nguyen and Lam Tien Do (2026). Impact of *Scutellonema curcumae* sp. n. (Nematoda: Hoplolaimidae) on the Phytochemical Profile and Biological Activities of Turmeric (*Curcuma longa* L.). *Molecules*, 31(6), 920.

2. **Dinh Thi Tu**, Ngo Kim Chi, Le Thi Thuy Huong, Do Huu Nghi, Pham Minh Quan (2026). *In silico* and *in vitro* investigation of curcuminoid as potential TLR4/MD-2 complex inhibitors using molecular docking and molecular dynamic simulations. *Vietnam Journal of Science and Technology*. https://doi.org/10.15625/2525-2518/24045.

3. Dinh Hieu Truong, **Thi Tu Dinh,** Thi My Duyen Trinh, Thi Hong Minh Pham, Minh Quan Pham, Urszula Gawlik-Dziki and Duy Quang Dao (2025). HOO radical scavenging activity of curcumin I and III in physiological conditions: a theoretical investigation on the influence of acid-base equilibrium and tautomerism. *RSC Advances*, 15(8), 5649-5664.

4. Phi Hung Nguyen, Anh Tuan Nguyen, **Thi Tu Dinh**, Dao Cuong To, Thi Phuong Hoang, Ngoc Quang Dang, Thi Thuy Do, Thi Ha Vu, Thi Thuc Bui, Thi Thu Ha Trinh (2023). Methodology for quick analysis of curcumin, demethoxycurcumin and bisdemethoxycurcumin from turmeric by Agilent 1260 HPLC system. *UD-JST*, *21*(5), 103-109.

1. Rationale

Turmeric (*Curcuma longa* L.) is a medicinally important plant belonging to the Zingiberaceae family, widely used in both traditional and modern medicine. The curcuminoid complex in turmeric rhizomes, comprising curcumin (CUR), demethoxycurcumin (DMC), and bisdemethoxycurcumin (BDMC), has been demonstrated to possess a diverse spectrum of biological activities: antioxidant, anti-inflammatory, cytotoxic against cancer cells, and antimicrobial.

However, several issues remain to be clarified: the individual efficacy of CUR, DMC, and BDMC on specific molecular targets has not been fully elucidated; the synthesis of hybrid derivatives between curcumin and other bioactive scaffolds (zerumbone, propargyl) to improve pharmacological properties remains a limited approach; the molecular-level mechanisms of action require further clarification using modern computational tools; and the impact of parasitic nematodes on medicinal plant quality has not been comprehensively assessed. Based on these considerations, this dissertation was conducted using a multidisciplinary approach, integrating synthetic chemistry, experimental pharmacology, *in silico* modeling, and nematode biology to comprehensively evaluate the medicinal value of Vietnamese turmeric. The dissertation is entitled: "**Isolation, purification of curcumin and semi-synthesis of its derivatives guided by *in vitro* and *in silico* biological activities from turmeric (*Curcuma longa* L.) in Vietnam".**

2. Research objectives

To investigate the chemical composition, synthesize novel derivatives, evaluate biological activities, and elucidate the mechanisms of action of curcuminoids and their derivatives from C. longa:

1. Isolation and structural elucidation of the three main curcuminoid components (CUR, DMC, BDMC) from turmeric rhizomes.

2. Semi-synthesis of hybrid curcumin-zerumbone and di-propargyl curcumin derivatives; structural characterization by modern spectroscopic methods and evaluation of their biological activities.

3. Evaluation of antioxidant (DPPH), anti-inflammatory (NO inhibition on RAW 264.7), cytotoxic (MTT on 5 cancer cell lines), and antimicrobial (MIC) activities of the compounds.

4. *In silico* studies: prediction of HOO• radical scavenging activity by DFT, elucidation of anti-inflammatory mechanisms via molecular docking

and molecular dynamics (MD) simulations with the TLR4/MD-2 complex, and ADMET pharmacokinetic profiling.

5. Description of the novel nematode species *Scutellonema curcumae* sp. n. parasitizing turmeric and assessment of its impact on curcuminoid content.

3. Research subjects and scope

Research subjects include: rhizomes of *C. longa* L. collected in Vietnam; three purified curcuminoid components (CUR, DMC, BDMC); semi-synthetic derivatives (curcumin-monozerumbone, curcumin-biszerumbone, di-propargyl curcumin); and root-parasitic nematodes. The scope encompasses chemical isolation, organic synthesis, *in vitro* bioactivity evaluation, *in silico* modeling, and biological classification of nematodes (morphological and molecular).

4. Novel contributions of the dissertation

1. First discovery and description of the novel nematode species *Scutellonema curcumae* sp. n. on Vietnamese turmeric roots. A correlation between nematode density and BDMC content and biological activity was established (SC_{50} decreased from 43.62 to 13.85 µg/mL with reduced nematode infestation).

2. Successful semi-synthesis of the hybrid derivative curcumin-monozerumbone (**4**), which enhanced lipophilicity (ClogP from 3.72 to 6.51) and improved biological activities: anti-inflammatory potency increased 3.8-fold compared to curcumin; cytotoxicity against hepatocellular carcinoma (Hep-G2) increased 2.5-fold; antimicrobial spectrum expanded, inhibiting 6/8 tested strains (versus 2/8 for curcumin).

3. Through molecular docking and MD simulations, the antioxidant and anti-inflammatory mechanisms were elucidated at the molecular level. BDMC was demonstrated to form more stable complexes with the TLR4/MD-2 protein (binding energy -9.73 kcal/mol versus -9.29 kcal/mol for curcumin), providing a molecular basis for interpreting the *in vitro* experimental results.

5. Dissertation structure

The dissertation comprises 112 pages, organized into 3 main chapters (in addition to the Introduction and Conclusions), with 19 tables, 27 figures, and 146 references.

CHAPTER 1. LITERATURE REVIEW

This chapter synthesizes the foundational knowledge on *C. longa*, including botanical characteristics, ecological distribution, chemical composition, and biological activities of curcuminoids.

1.1. Overview of the genus *Curcuma* L.

The genus Curcuma belongs to the Zingiberaceae family, comprising approximately 70-80 species of perennial rhizomatous herbs. These species are widely distributed in tropical Southeast Asia and the Asia-Pacific region. Modern medicine has recognized their broad spectrum of activities, including antioxidant, antiviral, antibacterial, and anti-inflammatory properties. To date, nearly 720 compounds have been identified, with sesquiterpenoids and diarylheptanoids as the principal constituents. The curcuminoid system (curcumin, demethoxycurcumin, and bisdemethoxycurcumin) is considered the most medicinally valuable group of compounds.

1.2. Overview of turmeric (*Curcuma longa* L.)

Turmeric originates from India and is now widely cultivated in tropical countries, with Vietnam being an important source region. In traditional Eastern medicine, turmeric is used for promoting blood circulation, treating gastric pain, menstrual irregularities, and wound healing. In India and Southeast Asian countries, it is also used for blood purification, treating colds, helminth infections, and dermatological conditions.

1.3. Structure and physicochemical properties of the curcuminoid system

The curcuminoid system accounts for approximately 2–8% of dried turmeric rhizome mass, comprising three principal components that always coexist. All three derivatives belong to the diarylheptanoid class with a basic scaffold consisting of two aromatic rings connected by a 7-carbon chain. The key structural difference lies in the methoxy (-OCH_3) substituents on the aromatic rings: curcumin (CUR): 2 methoxy groups (60-70%); demethoxycurcumin (DMC): 1 methoxy group (20-27%); bisdemethoxycurcumin (BDMC): no methoxy groups (10-15%). Despite being the least abundant, BDMC exhibits superior physicochemical

stability: its melting point reaches 222°C, significantly higher than CUR (184°C) and DMC (172°C). Under harsh conditions (alkaline, thermal, oxidative), the stability order is established as BDMC > DMC > CUR.

1.4. Biological activities and specific molecular mechanisms

Current research is increasingly focused on BDMC due to its valuable pharmacological mechanisms: BDMC demonstrates superior inhibition of iNOS enzyme compared to curcumin; BDMC acts as a GPR161 receptor inhibitor, blocking the mTOR signaling pathway and promoting apoptosis in cancer cells (particularly triple-negative breast cancer). Due to lower degradation rates, BDMC maintains therapeutic concentrations in tissues longer than CUR, overcoming the rapid elimination disadvantage of the principal derivative.

1.5. *In silico* research methods

The dissertation applies modern computational tools for atomic-level mechanism elucidation: quantum chemical calculations (DFT) using Gaussian 16 with the M06-2X functional to investigate antioxidant mechanisms through thermodynamic parameters (BDE, IP, PA); molecular simulations (Docking & MD) using AutoDock and GROMACS to evaluate interactions between curcuminoids and protein targets such as iNOS and TLR4/MD-2.

1.6. Parasitic nematodes and their impact on medicinal plant quality

Root nematodes (particularly the genera *Scutellonema* and *Meloidogyne*) are hazardous pests that not only reduce yields but also cause biological stress, disrupting curcuminoid accumulation. Nematode management is essential for standardizing raw material zones and ensuring curcuminoid content and biological activity.

CHAPTER 2. MATERIALS AND METHODS

2.1. Curcuminoid derivative synthesis

2.1.1. Curcumin-zerumbone derivatives

Semi-synthesis was performed in two stages: (i) Bromination of zerumbone with NBS in CH_3CN:H_2O (1:1), yielding 3-bromozerumbone (> 95% yield); (ii) Nucleophilic substitution of curcumin with 3-bromozerumbone using K_2CO_3 base in DMF, at room temperature, for 24 h. Purification by column chromatography and semi-preparative HPLC

afforded curcumin-monozerumbone (15% yield) and curcumin-biszerumbone (11% yield). Structures were determined by ^{1}H-NMR, ^{13}C-NMR, and HR-MS.

2.1.2. Di-propargyl curcumin derivative

Synthesis was performed via Williamson ether synthesis: curcumin reacted with propargyl bromide (2.5 equiv.), K_2CO_3 (3.0 equiv.) in anhydrous DMF, room temperature, 24 h. Di-propargyl curcumin ($C_{27}H_{24}O_6$, 21% yield) was characterized by NMR and HR-MS.

2.2. *In vitro* biological activity evaluation

Four assay groups were conducted: (i) Antioxidant activity by the DPPH method (λ = 517 nm, positive control: ascorbic acid); (ii) Anti-inflammatory activity via NO inhibition on RAW 264.7 cells stimulated with LPS (Griess reagent, λ = 540 nm); (iii) Cytotoxicity against 5 human cancer cell lines (Hep-G2, HeLa, MCF-7, A549, HGC-27) by the MTT assay (positive control: Paclitaxel); (iv) Antimicrobial activity by broth microdilution MIC determination on 4 bacterial and 4 fungal strains.

2.3. *In silico* studies

HOO• radical scavenging activity was predicted by DFT (M06-2X/6-311++G(3df,3pd)) in aqueous and lipid (PEA) environments, examining three mechanisms: HAT (Abs), RAF (Add), and SET. Anti-inflammatory mechanisms were elucidated by molecular docking (AutoDock 4.2.6, LGA) and molecular dynamics simulations (GROMACS, Amber99SB-iLDN/GAFF) with the TLR4/MD-2 complex (PDB: 2Z64, 3VQ2). ADMET profiles were evaluated using Molinspiration, ProTox-II, and admetSAR.

2.4. Nematode research

Nematodes were isolated using the modified Baermann tray method. Identification was based on morphology (Olympus BX51 microscope) combined with molecular biology (sequencing of D2-D3/28S rDNA, ITS, and COI mtDNA regions; phylogenetic analysis using MrBayes). The impact of nematode infestation on curcuminoid content was quantified by HPLC (Agilent 1260, Eclipse XDB-C18 column, λ = 428 nm).

CHAPTER 3. RESULTS AND DISCUSSION

3.1. Isolation and structural characterization

Three principal curcuminoid compounds were successfully isolated from Vietnamese turmeric rhizomes (*C. longa* L.): curcumin (CUR), the main compound with a symmetrical structure bearing two methoxy groups; demethoxycurcumin (DMC), the intermediate compound containing one methoxy group; and bisdemethoxycurcumin (BDMC), the simplest structure without methoxy groups. These compounds were isolated with high purity through modern chromatographic methods and structurally characterized by ^{1}H-NMR and ^{13}C-NMR spectroscopy, with data consistent with literature reports.

3.1.1. Curcumin (CUR)

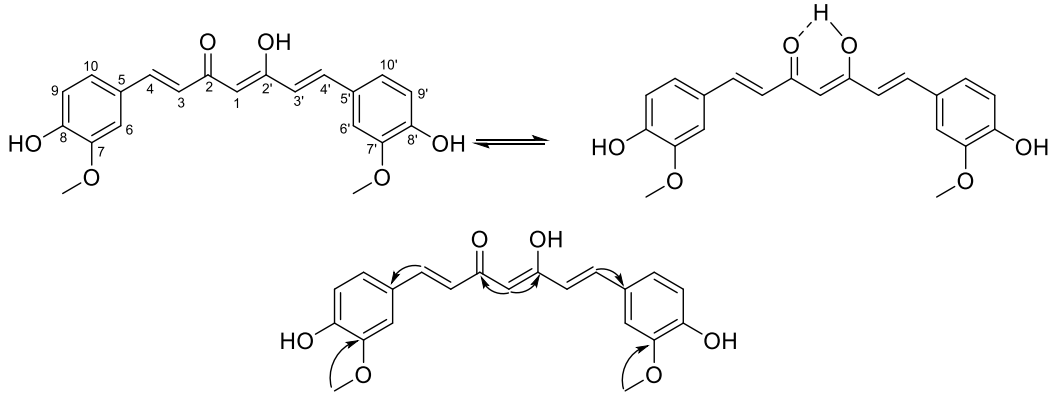

Figure 3.1. Chemical structure of the CUR compound isolated from turmeric

Table 3.1. ^{1}H and ^{13}C-NMR spectral data for compound CUR

No	CUR		[144]	
	$^{a}\delta_C$ ppm	**$^{a}\delta_H$ ppm (*J*; Hz)**	**#δ_C ppm**	**#δ_H ppm (*J*; Hz)**
1	101,1	5,80 (s)	100,9	5,98 (s)
2, 2′	183,3	-	183.4	16.41 (s)
3, 3′	121,8	6,49 (d; 15,6)	121,1	6,73 (d; 16,0)
4, 4′	140,6	7,60 (d; 15,6)	140,7	7,53 (d; 16,0)
5, 5′	127,7	-	126,4	-
6, 6′	109,7	7,04 (s)	111,4	7,32 (d; 2,0)
7, 7′	146,8	-	148,0	-
8, 8′	147,9	-	149,4	9,74 (s)
9, 9′	114,9	6,94 (d; 8,4)	115,7	6,85 (d; 8,1)
10, 10′	122,9	7,12 (d; 6,6)	123,2	7,16 (dd; 2,0; 8,1)
OCH_3	56,0	3,94 (s)	55,7	3,84 (s)
-OH	-	5,89 (1H, br s)		

[a]$CDCl_3$ at 600 MHz (^{1}H-NMR) and 150 MHz (^{13}C-NMR)
[#] DMSO-d_6 at 500 MHz (^{1}H-NMR) and 125 MHz (^{13}C-NMR)

3.1.2. Demethoxycurcumin (DMC)

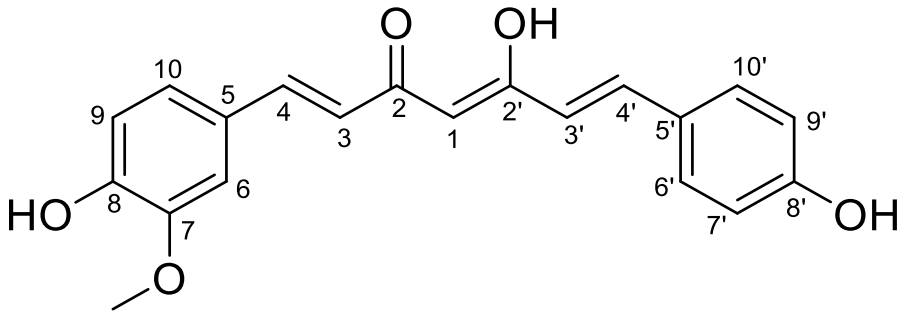

Figure 3.2. Chemical structure of the DMC compound isolated from turmeric

Table 3.2. ^{1}H and ^{13}C-NMR spectral data for compound DMC

No	DMC		[145]	
	[a]δ_C ppm	**[a]δ_H ppm (*J*; Hz)**	**#δ_C ppm**	**#δ_H ppm (*J*; Hz)**
1	100,9	5,82 (s)	102,0	5,98 (s)
2	183,3	-	184,8	-
3	121,1	6,53 (dd; 15,5; 3,0)	122,3	6,64 (d; 15,8)
4	140,7	7,63 (d; 15,5)	142,1	7,59 (d; 15,8)
5	126,4	-	128,6	-
6	111,2	7,09 (d; 2,0)	111,7	7,23 (d; 1,9)
7	148,0	-	149,4	-
8	149,3	-	150,5	-
9	115,7	6,97 (d, 8,5)	116,9	6,84 (d, 8,2)
10	125,9	7,16 (dd; 8,5; 2,0)	124,1	7,12 (dd; 8,2; 1,9)
2′	183,1	-	184,8	-
3′	123,2	6,53 (dd; 15,5; 3,0)	122,3	6,61 (d, 15,6)
4′	140,4	7,63 (d; 15,5)	142,1	7,59 (d, 15,8)
5′	127,9	-	128,0	-
6′	130,4	7,51 (d, 8,5)	131,5	7,51 (d, 8,7)
7′	116,0	6,89 (d, 8,5)	116,6	6,84 (d, 8,2)
8′	159,8	-	161,1	-
9′	116,0	6,89 (d; 8,5)	116,6	6,84 (d; 8,2)
10′	130,4	7,51 (d; 8,5)	131,5	7,51 (d; 8,7)
7-OCH_3	56,4	3,95 (s)	56,5	3,93 (s)
-OH		5,89 (s)		

[a] $CDCl_3$ at 600 MHz (^{1}H-NMR) and 150 MHz (^{13}C-NMR)
[#] Methanol-d_4 at 500 MHz (^{1}H-NMR) and 125 MHz (^{13}C-NMR)

3.1.3. Bisdemethoxycurcumin (BDMC)

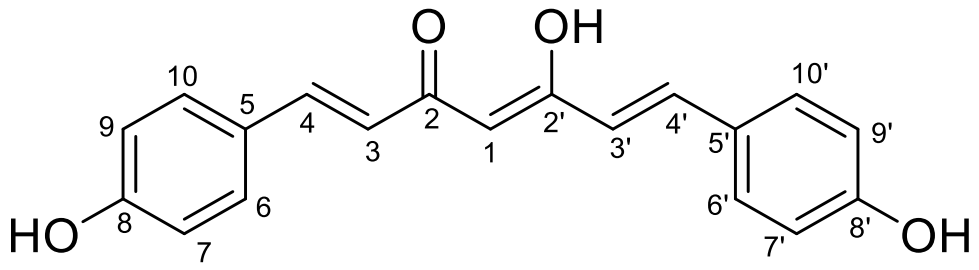

Figure 3.3. Chemical structure of BDMC compound isolated from turmeric

Table 3.3. ^{1}H and ^{13}C-NMR spectral data for compound BDMC

No	BDMC		[145]	
	[a]δ_C ppm	**[a]δ_H ppm (*J*; Hz)**	**#δ_C ppm**	**#δ_H ppm (*J*; Hz)**
1	100,9	5,80 (1H, s)	101,9	5,94 (2H, s)
2, 2′	183,2	-	184,8	-
3, 3′	120,8	6,53 (2H; d; 15,5)	122,0	6,60 (2H; d; 15,8)
4, 4′	140,4	7,62 (2H; d; 15,5)	141,8	7,58 (2H; d; 15,8)
5, 5′	125,9	-	128,0	-
6, 6′, 10, 10′	130,3	7,48 (4H; d, 8,5)	131,1	7,49 (4H; d, 8,6)
7, 7′, 9, 9′	115,9	6,87 (4H; d; 8,5)	116,9	6,83 (4H; d; 8,6)
8, 8′	159,8	-	161,1	-

[a] $CDCl_3$ at 500 MHz (^{1}H-NMR) and 150 MHz (^{13}C-NMR)
[#] DMSO-d_6 at 500 MHz (^{1}H-NMR) and 125 MHz (^{13}C-NMR)

3.2. Novel nematode species *Scutellonema curcumae* sp. n. and its impact on turmeric chemistry and bioactivity

3.2.1. Taxonomy, molecular characteristics, and ecology

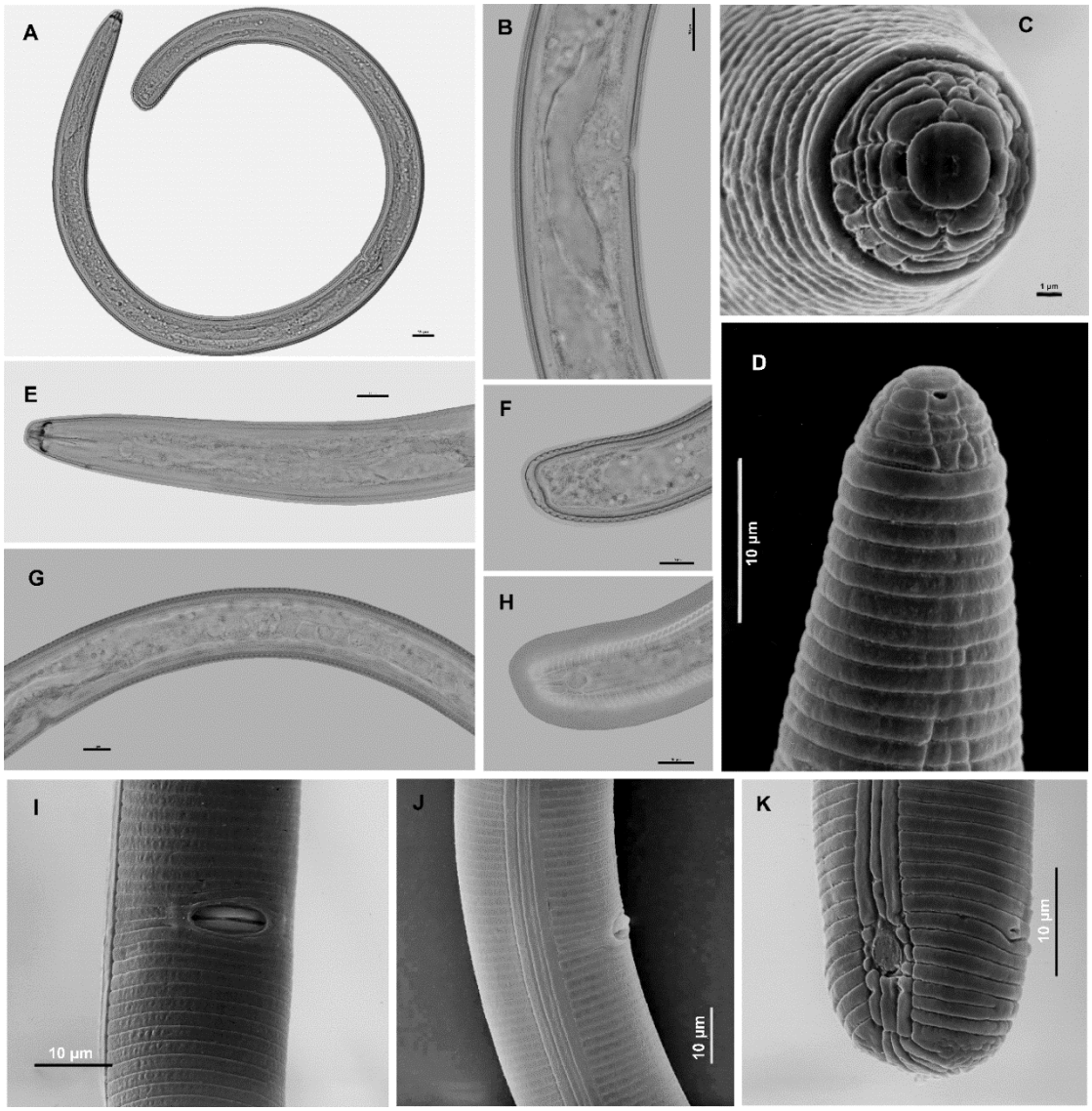

Figure 3.4. Female of *S. curcumae* sp. n. from Vietnam**.** A: Entire body; B: Vulval region; C: Anterior region (head region); D: Tail region; E: Ovary; F: Tail region showing scutella (large phasmids). (Scale bars: A: 20 µm; B-F: 10 µm)

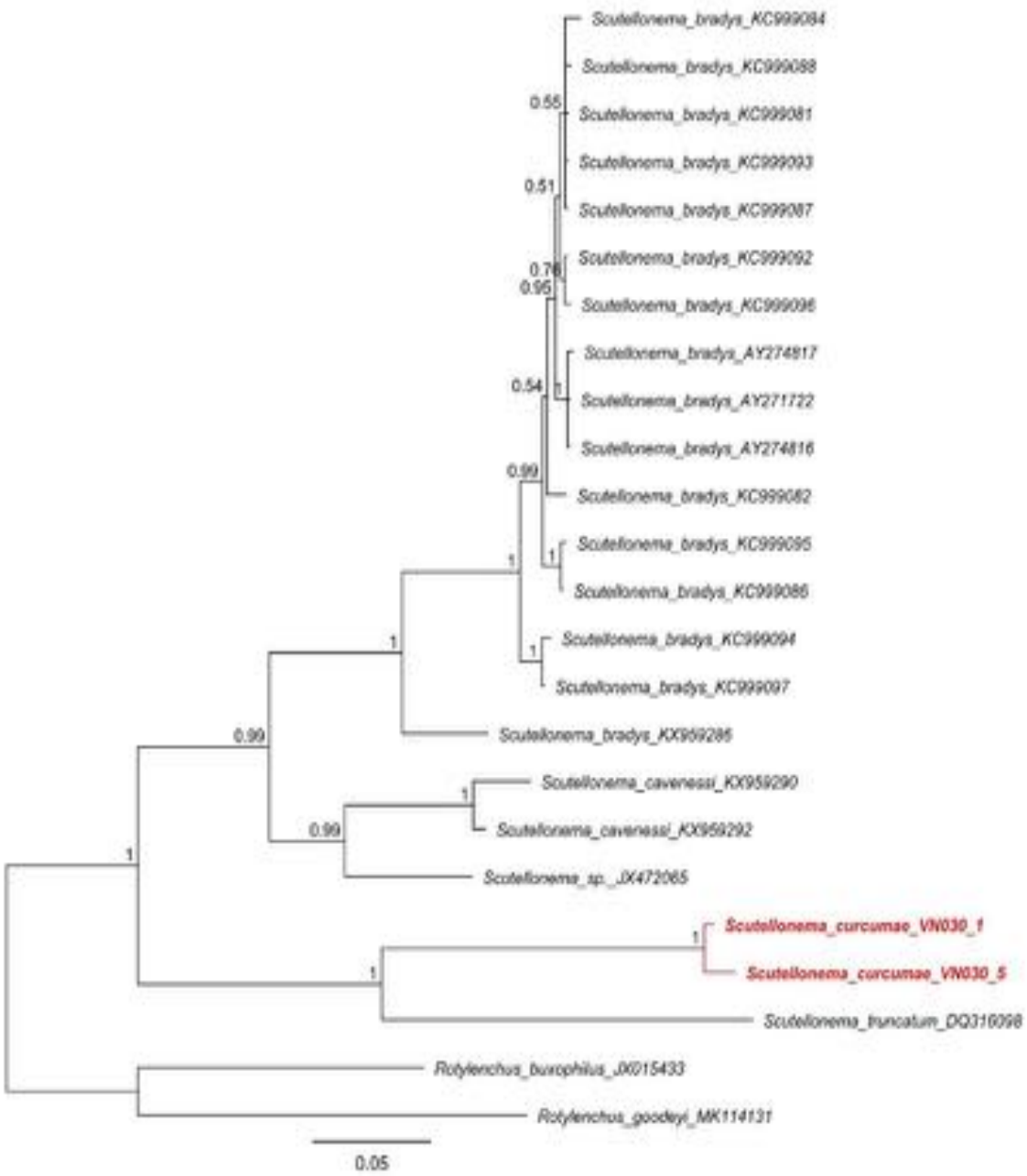

Figure 3.5. Bayesian phylogenetic tree constructed using ITS sequences of *Scutellonema* species under the GTR+G+I model. The sequence of *S. curcumae* sp. n. is indicated in bold and red font.

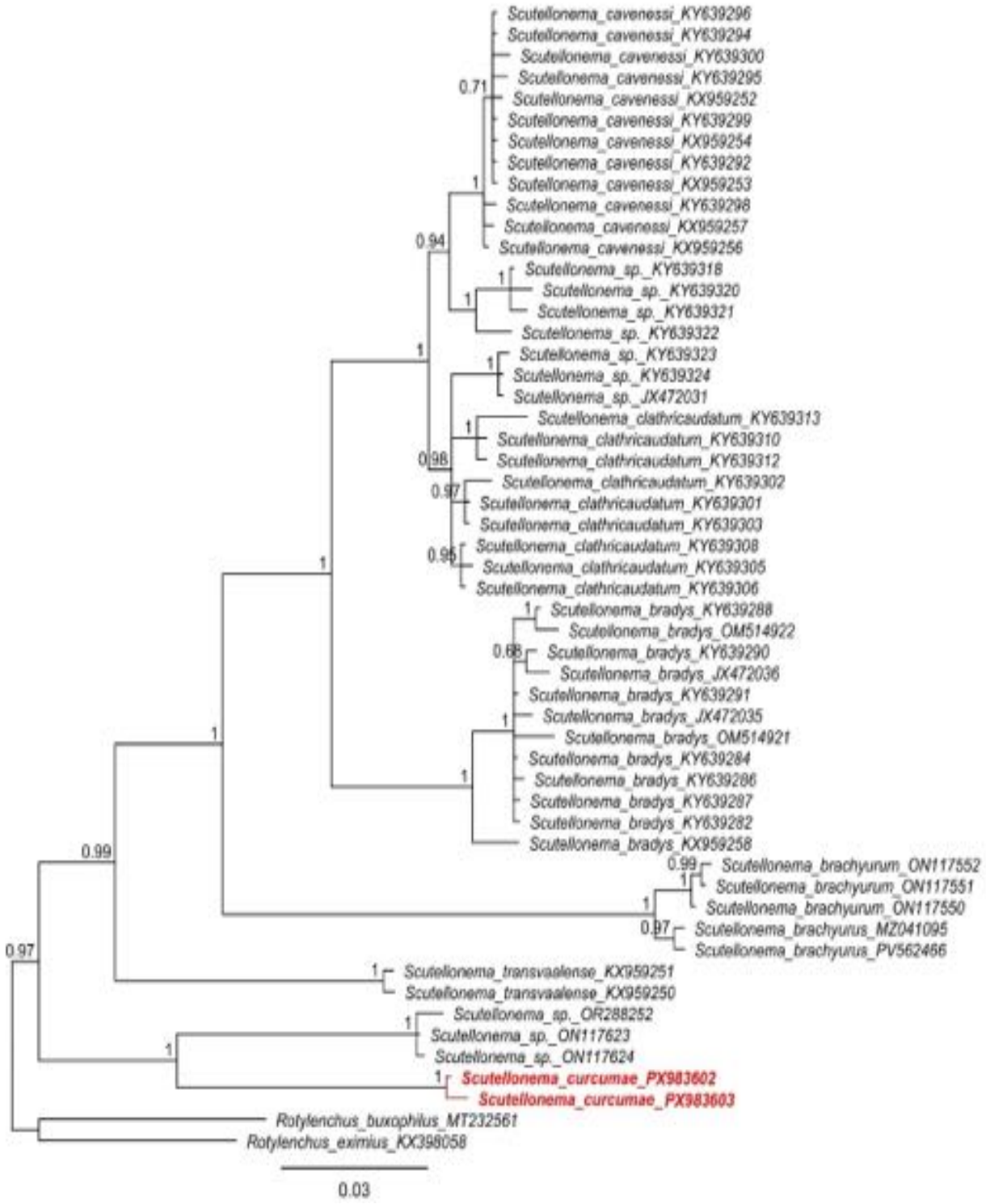

Figure 3.6. Bayesian phylogenetic tree constructed using D2-D3 sequences of *Scutellonema* species under the GTR+G+I model. The sequence of *S. curcumae* sp. n. is indicated in bold and red font.

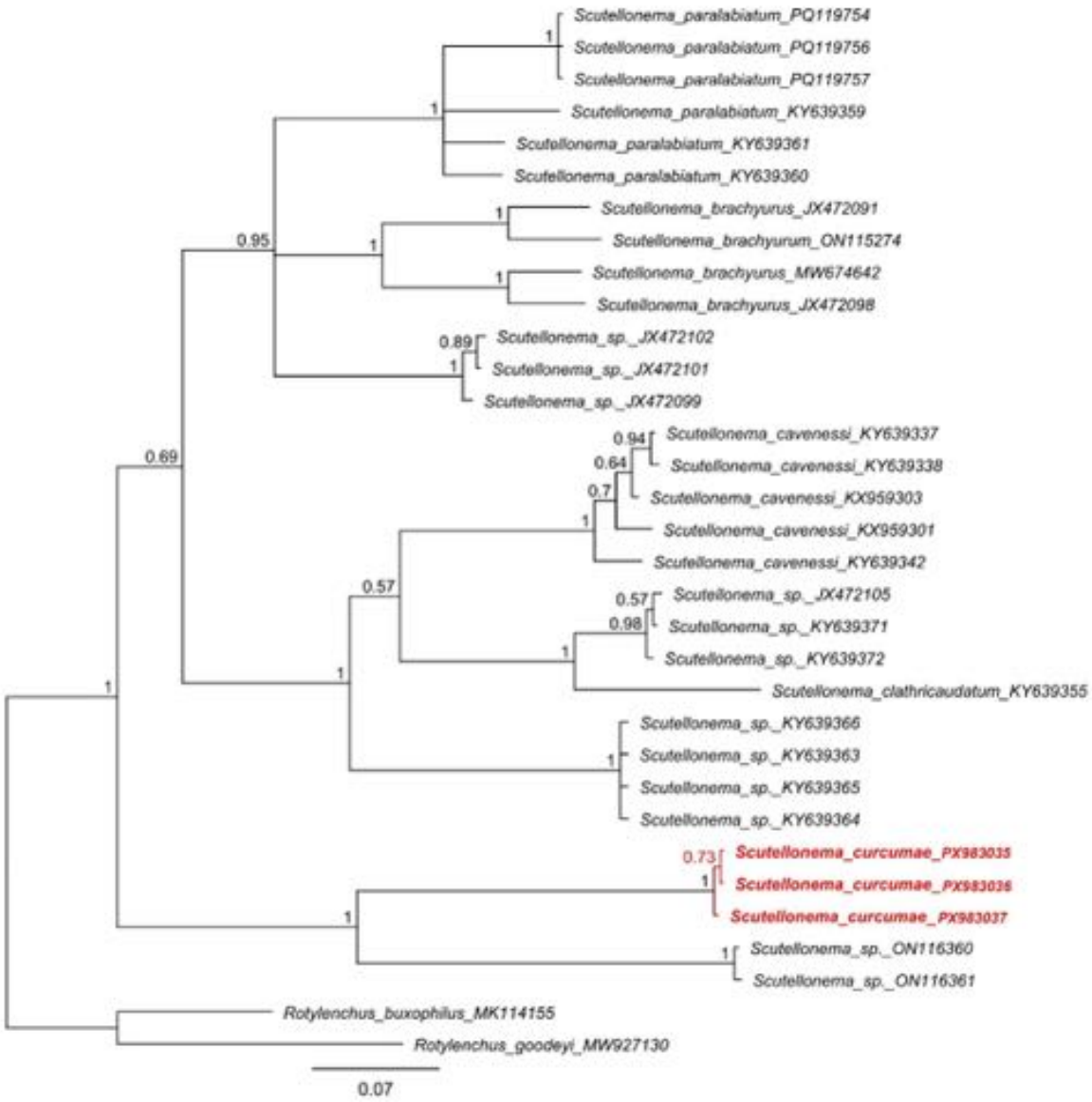

Figure 3.7. Bayesian phylogenetic tree constructed using COI sequences of *Scutellonema* species under the GTR+G+I model. The sequence of *S. curcumae* sp. n. is indicated in bold and red font.

A major scientific contribution of this dissertation is the discovery and description of a novel plant-parasitic nematode species, *Scutellonema curcumae* sp. n. Morphological examination under light and scanning electron microscopy revealed characteristic features: a spiral body posture at rest, a well-developed stylet (mean length 32 μm) enabling penetration of the hard turmeric tissues, and notably large scutella positioned symmetrically on both sides of the body at the anal level. Molecular identification using ITS, 28S, and COI gene markers confirmed the finding. Bayesian phylogenetic analysis showed that *S. curcumae* sp. n. forms a distinct clade, closely related to but clearly differentiated from *S. truncatum*.

3.2.2. Changes in curcuminoid content due to nematode infestation

Table 3.5. Physicochemical composition and nematode density in turmeric and cultivation soil

Symbols	**Sample type**	**pH**	**Soil moisture (%)**	**Total nitrogen content (%)**	**Total nematode density in soil (individuals/100 g dry soil)**	***S. curcumae* sp. n. density (individuals/100 g dry soil)**
M1	Curcuma	-	-	-	59,7	19,6
	Soil	6,5	73,5	1,05	131,8	25,3
M2	Curcuma	-	-	-	17,7	7,5
	Soil	6,3	73,4	0,92	58,2	11,4
M3	Curcuma	-	-	-	88,4	10,7
	Soil	6,6	73,6	0,95	79,3	3,8
M4	Curcuma	-	-	-	78,4	12,5
	Soil	7,1	74,1	0,98	185,3	27,9
M5	Curcuma	-	-	-	58,4	16,5
	Soil	6,8	74,2	1,07	125,3	29,6
M6	Curcuma	-	-	-	66,8	12,3
	Soil	6,9	74,0	1,01	141,5	22,1
M7	Curcuma	-	-	-	33,9	8,2
	Soil	6,0	72,8	0,90	87,6	5,5
M8	Curcuma	-	-	-	47,9	3,1
	Soil	6,2	72,9	0,91	90,2	6,3
M9	Curcuma	-	-	-	23,3	1,6
	Soil	5,9	72,8	0,95	70,1	4,5
M10	Curcuma	-	-	-	11,3	0,8
	Soil	5,6	70,9	0,92	36,8	2,6

Table 3.6. Chemical composition and biological activity of turmeric rhizomes

Sample	**curcuminoid (%)**	**CUR (%)**	**DMC (%)**	**BDMC (%)**	**SC_{50} (µg/ml)**	**IC_{50} on HepG2 (µg/ml)**	**IC_{50} on A549 (µg/ml)**
	Ascorbic acid				6,81 ± 1,03		
	Paclitaxel					47,2 ± 1.26 nM	21,3 ± 1.03
M1	4,01 ± 0,05	3,19 ± 0,08	0,64 ± 0,04	0,16 ± 0,01	43,62 ± 3,08	44,23 ± 2,08	55,23 ± 3,34
M2	4,25 ± 0,03	3,07 ± 0,07	0,86 ± 0,02	0,32 ± 0,03	23,45 ± 2,19	43,67 ± 2,86	58,93 ± 2,99
M3	4,16 ± 0,04	3,06 ± 0,05	0,80 ± 0,03	0,31 ± 0,02	21,03 ± 2,56	45,37 ± 3,49	60,32 ± 3,05
M4	4,15 ± 0,02	3,18 ± 0,05	0,72 ± 0,02	0,23 ± 0,01	32,89 ± 3,55	38,82 ± 2,98	52,75 ± 2,45
M5	4,10 ± 0,04	3,19 ± 0,06	0,69 ± 0,04	0,21 ± 0,02	40,31 ± 3,86	37,85 ± 2,05	50,37 ± 2,97
M6	4,15 ± 0,05	3,21 ± 0,06	0,69 ± 0,01	0,23 ± 0,01	34,26 ± 3,82	38,63 ± 2,52	51,34 ± 3,14
M7	4,23 ± 0,03	3,16 ± 0,09	0,74 ± 0,02	0,31 ± 0,03	25,87 ± 2,44	39,38 ± 1,56	48,21 ± 3,82
M8	4,70 ± 0,06	3,38 ± 0,07	0,91 ± 0,03	0,41 ± 0,02	18,91 ± 1,73	35,76 ± 2,88	47,55 ± 2,43
M9	4,88 ± 0,07	3,45 ± 0,08	0,98 ± 0,04	0,46 ± 0,01	16,42 ± 1,89	29,04 ± 1,22	41,43± 3,02
M10	4,95 ± 0,02	3,45 ± 0,04	0,90 ± 0,02	0,56 ± 0,02	13,85 ± 1,31	29,35 ± 1,10	40,37 ± 3,31

Curcuminoid content variations significantly affected turmeric bioactivity. In samples with low nematode pressure, increased curcuminoid content led to markedly enhanced antioxidant activity (SC_{50} decreased from

43.62 to 13.85 µg/mL). Similarly, cytotoxic activity improved substantially, with IC_{50} values decreasing from 44.23 to 29.35 µg/mL for hepatocellular carcinoma cells (Hep-G2) and from 55.23 to 40.37 µg/mL for lung cancer cells (A549).

3.3. Semi-synthesis of curcumin derivatives

3.3.1. Curcumin-zerumbone semi-synthesis

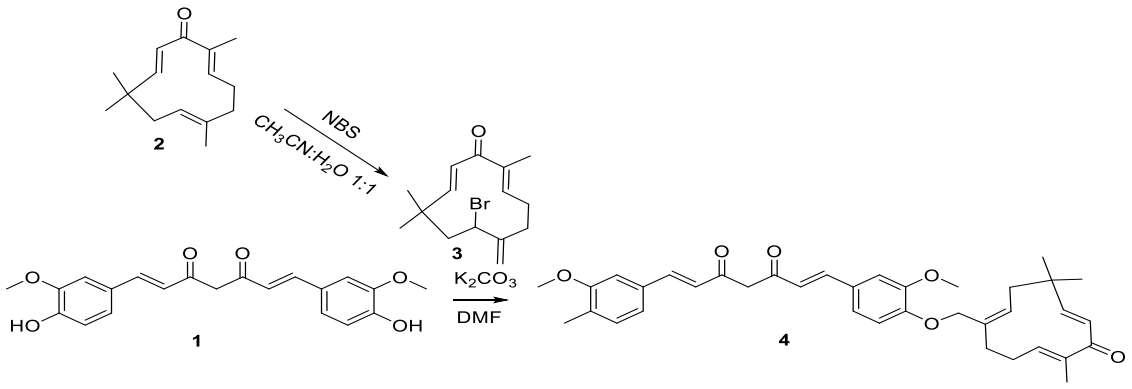

Figure 3.8. Synthesis of CUR derivatives isolated from turmeric rhizomes

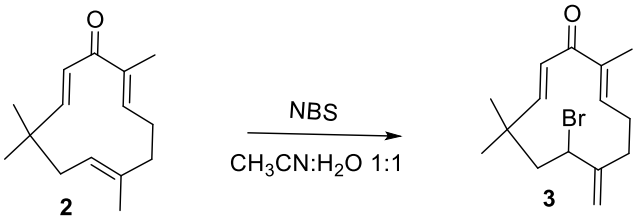

Figure 3.9. Synthesis of curcumin derivatives - Stage 1

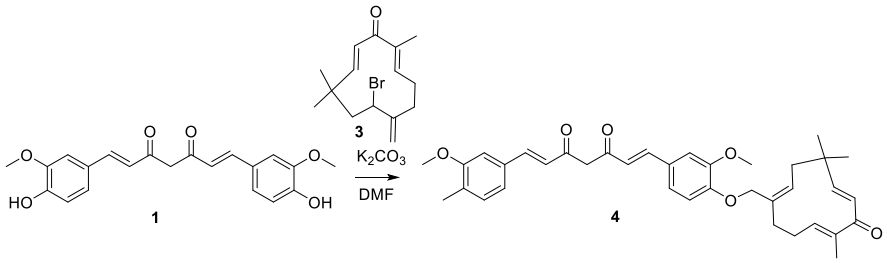

Figure 3.10. Synthesis of curcumin derivatives - Stage 2

Two novel derivatives were successfully synthesized: curcumin-monozerumbone (mp: 118-120 °C, 15% yield) and curcumin-biszerumbone (mp: 138-140 °C, 11% yield). Structures were confirmed by ^{1}H-NMR, ^{13}C-NMR, and HR-MS. For compound **4**, the ^{1}H-NMR spectrum showed a single phenolic -OH proton signal at δ_H 9.64 (1H, s), confirming that ether substitution occurred at only one phenol end of the curcumin molecule, breaking the original symmetry. The two methoxy groups appeared as two separate singlets at δ_H 3.84 (3H, s) and 3.81 (3H, s). Zerumbone-characteristic methyl protons were observed at δ_H 1.67, 1.22, and 1.05 (each

3H, s). The ^{13}C-NMR spectrum displayed two separate carbonyl signals at δ_C 183.7 and 182.6 ppm, consistent with the loss of molecular symmetry.

For compound **5**, the restored high symmetry was confirmed by the disappearance of the phenolic –OH signal, the methoxy groups merging into a single signal at δ_H 3.84 (6H, s), and all zerumbone-characteristic signals showing doubled integrals: δ_H 1.67 (6H, s), 1.22 (6H, s), 1.05 (6H, s), confirming the attachment of exactly two zerumbone moieties.

3.3.2. Di-propargyl curcumin semi-synthesis

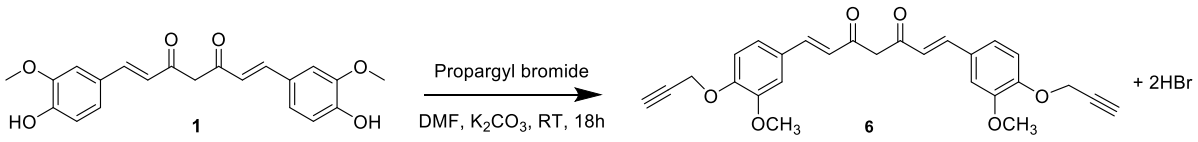

Figure 3.11. Synthesis of curcumin Di-propargyl

Compound **6** was obtained as a yellow powder (21% yield). Successful propargylation was confirmed by characteristic signals: methylene (–OCH_2–) at δ_H 4.89 (4H, d, J = 2.4 Hz) and terminal alkyne (–C≡CH) at δ_H 3.61 (2H, t, J = 2.4 Hz). The curcumin scaffold retained its trans configuration with alkene protons at δ_H 7.66 and 7.07 (J = 15.6 Hz) and symmetrical methoxy at 3.87 (6H, s).

3.3.3. Anti-inflammatory activity of curcumin derivatives

Table 3.7. NO production inhibitory activity and survival rate of RAW 264.7 cells treated with curcumin and its derivatives.

No	**Sample symbols**	**Compound name**	**IC_{50}** (μg/ml)	**Cell survival rate %**
1	CUR	Curcumin	121,06 ± 2,16	82,5 ± 2,1
2	**6**	Dipropargyl curcumin	85,40 ± 1,85	86,4 ± 1,8
3	**5**	Curcumin-biszerumbone	68,20 ± 1,50	88,2 ± 2,4
4	**4**	Curcumin-monozerumbone	32,15 ± 1,20	92,1 ± 1,5
5	Control sample	Cardamonin	0,61 ± 0,24	95,0 ± 1,2

Anti-inflammatory activity was evaluated via NO inhibition on RAW 264.7 macrophages stimulated with LPS. Curcumin-monozerumbone (**4**) exhibited the strongest anti-inflammatory activity with IC_{50} = 32.15 ± 1.20 µg/mL, approximately 3.8-fold more potent than CUR (121.06 ± 2.16 µg/mL). Curcumin-biszerumbone (**5**) also showed considerable activity (IC_{50} = 68.20 ± 1.50 µg/mL) but was less potent than the mono-derivative, likely due to steric hindrance from the two bulky zerumbone moieties.

3.3.4. Cytotoxic activity of curcumin derivatives

Cytotoxicity was evaluated on five human cancer cell lines. All semi-synthetic derivatives showed significantly improved activity compared to parent curcumin. Compound **4** exhibited the strongest cytotoxicity across all cell lines, with IC_{50} values of 25.35 (Hep-G2), 22.42 (HeLa), 28.05 (MCF-7), 31.25 (A549), and 26.60 (HGC-27) µg/mL, representing 2.0–2.6-fold improvements over CUR.

Table 3.8. IC50 values (µg/ml) of curcumin and its synthetic derivatives on 5 cancer cell lines

No	**Symbols**	**IC_{50} (µg/ml)**				
		Hep-G2	**HeLa**	**MCF-7**	**A549**	**HGC-27**
1	CUR	62,45 ± 2,15	58,15 ± 1,90	65,60 ± 2,35	72,20 ± 2,50	60,85 ± 2,05
2	**4**	25,35 ± 1,20	22,42 ± 1,15	28,05 ± 1,35	31,25 ± 1,50	26,60 ± 1,25
3	**5**	38,62 ± 1,55	35,30 ± 1,45	41,85 ± 1,70	45,45 ± 1,85	39,20 ± 1,60
4	**6**	48,15 ± 1,80	45,45 ± 1,65	52,60 ± 1,95	56,80 ± 2,10	49,35 ± 1,75
5	Paclitaxel	0,85 ± 0,05	0,68 ± 0,04	0,92 ± 0,05	1,15 ± 0,08	0,80 ± 0,05

3.3.5. Antimicrobial activity of curcumin derivatives

Curcumin-monozerumbone (**4**) displayed the broadest and strongest antimicrobial spectrum, inhibiting 6/8 tested strains. This compound was

active against Gram-positive bacteria and *C. albicans* (MIC = 100 μg/mL), and showed inhibition of *S. cerevisiae*, *A. niger*, and *E. coli* (MIC = 200 μg/mL), compared to curcumin which only inhibited 2/8 strains.

Table 3.9. Results of antimicrobial activity testing of curcumin and its derivatives, sample concentrations

Sample symbol	**Minimum inhibitory concentration (MIC: μg/ml)**							
	Gr (-)		**Gr (+)**		**Mold**		**Yeast**	
	E. coli	*P. aeruginosa*	*B. subtillis*	*S. aureus*	*A. niger*	*F. oxysporum*	*S. cerevisiae*	*C. albicans*
CUR	> 200	> 200	200	200	> 200	> 200	> 200	> 200
6	200	> 200	100	100	> 200	> 200	200	200
5	200	> 200	100	100	> 200	> 200	> 200	> 200
4	200	>200	100	100	200	> 200	200	100

Values > 200 μg/ml are considered inactive at the tested concentration

3.4. *In silico* simulation results

On the RAW 264.7 cellular model stimulated by LPS, BDMC demonstrated superior NO inhibition (IC_{50} = 91.22 μM) compared to CUR (121.06 μM). Molecular docking revealed that BDMC generates lower binding energy (−9.73 kcal/mol) and forms more stable hydrogen bonding interactions with amino acid residues in the binding cavity of TLR4/MD-2 compared to CUR (−9.29 kcal/mol).

Quantum kinetic (DFT) calculations demonstrated that BDMC possesses a HOO• radical scavenging rate constant in the lipid membrane environment approximately 20-fold higher than conventional curcumin, attributable to its flexible molecular structure and the absence of sterically hindering methoxy groups. ADMET predictions confirmed that BDMC has favorable pharmacokinetic properties, low toxicity (classes 4 and 5), and high absorption potential.

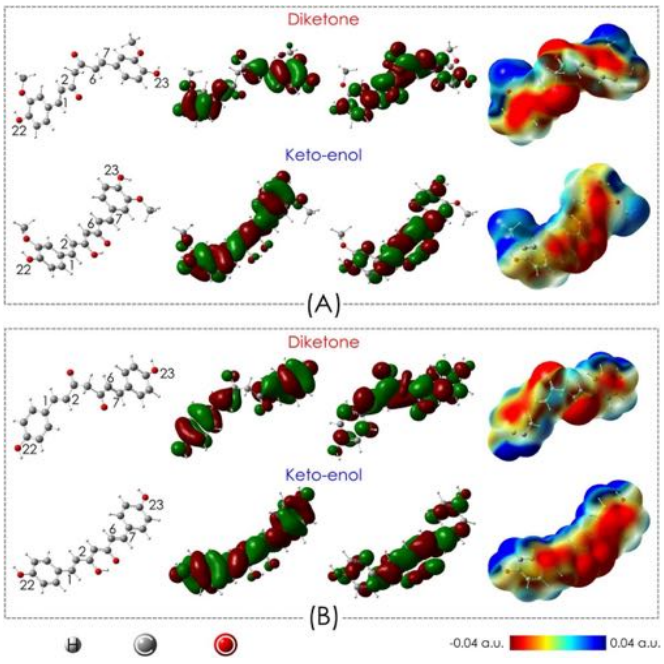

Figure 3.12. Optimized geometric structures, HOMO, LUMO, and electrostatic potential (ESP) maps of the diketone and keto-enol tautomers of CUR (A) and BDMC (B) in water.

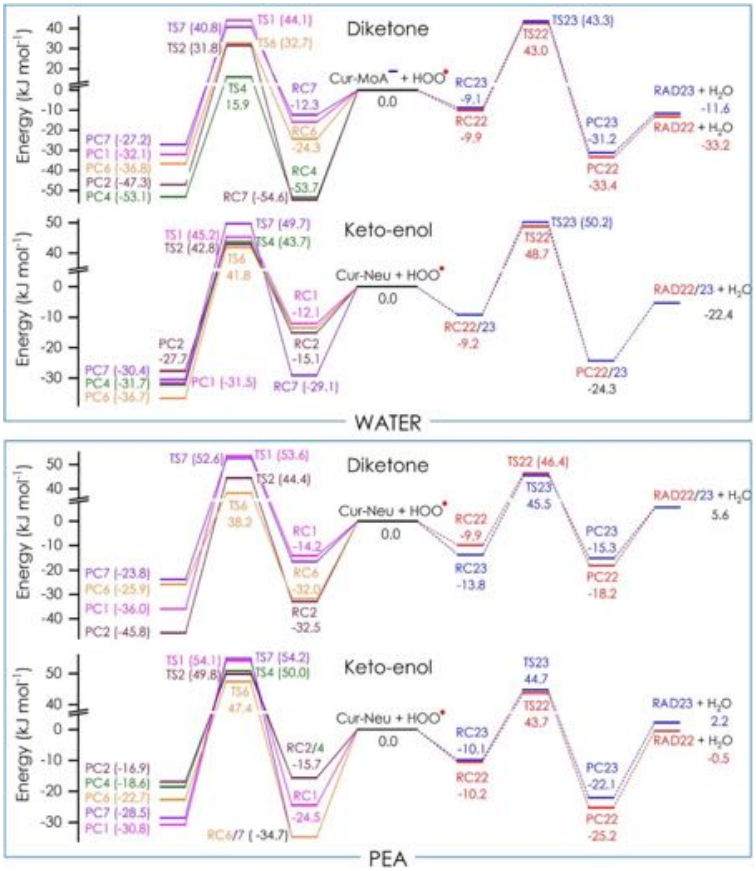

Figure 3.14. Relative enthalpy profile corrected for Zero Point Energy (ZPE) at 0 K for abstraction (right) and addition (left) reactions initiated by the HOO. radical of CUR in water and PEA.

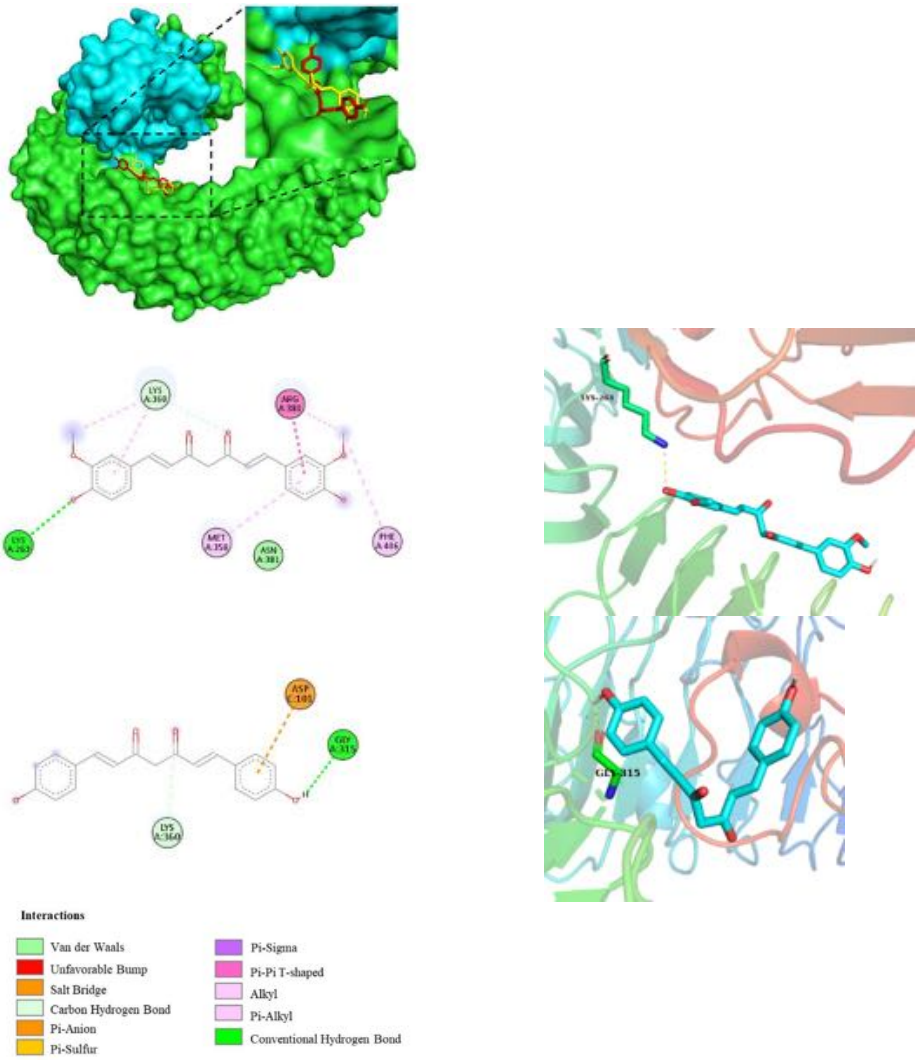

Figure 3.15. Interactions of CUR and BDMC within the TLR4/MD-2 complex obtained using AutoDock4. (A) The investigated compounds bind to a region on TLR4, adjacent to its interface with MD-2: CUR in red, BDMC in yellow; (B) Docking pose of CUR; (C) Docking pose of BDMC

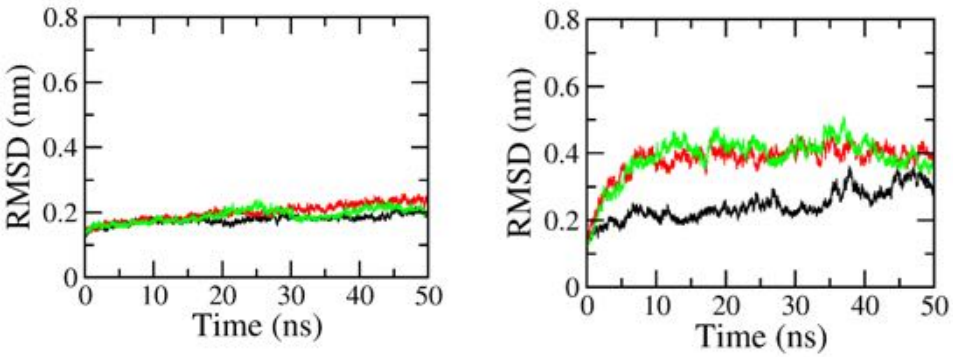

CUR **BDMC**

Figure 3.16. All-atom RMSD of TLR4/MD-2 with CUR (A) and BDMC (B) over three independent 50 ns MD simulation runs

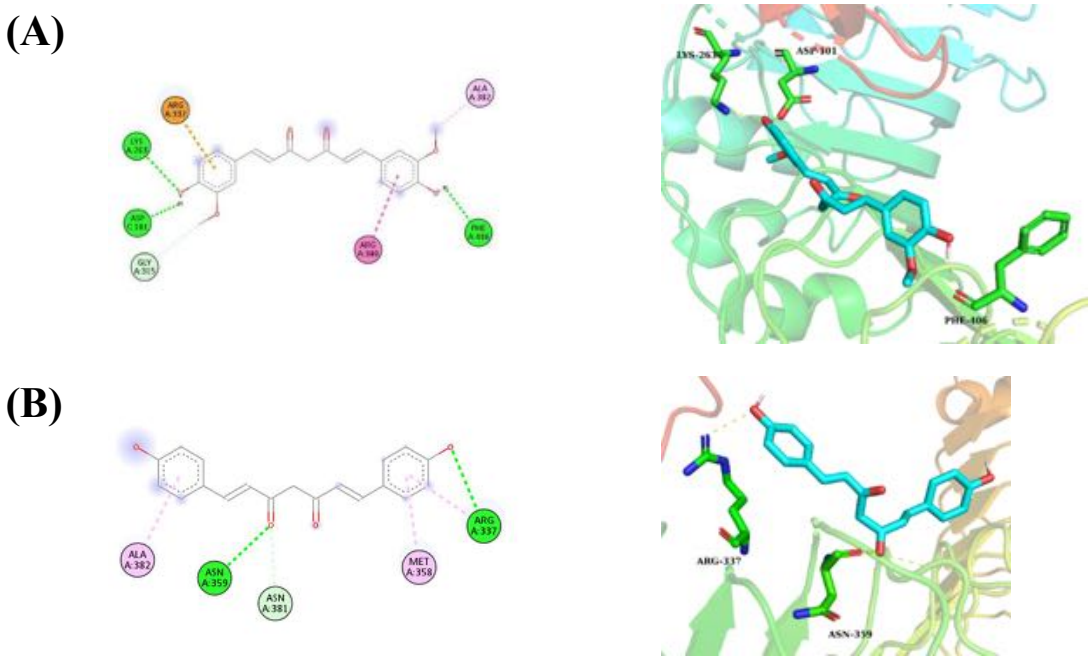

Figure 3.17. MD-refined binding poses of CUR (A) and BDMC (B) with TLR4/MD-2, obtained by clustering equilibrium snapshots of the complex with a 0.2 nm cutoff

Both CUR and BDMC possess optimal physicochemical properties for oral absorption, fully complying with Lipinski's Rule of Five without any violations. The consistency among pharmacokinetic models, MD simulation results, and affinity scores from AutoDock4 confirms that these natural derivatives are potential TLR4/MD-2 inhibitors with feasible pharmacological properties. Furthermore, their classification into toxicity classes 4 and 5, accompanied by favorable predicted LD_{50} values, indicates that these compounds possess a wide safety window, supporting the advancement of subsequent drug development studies.

Table 3.16. ADMET indices and toxicity predictions of potential compounds

Compound	**MW**	**HBD**	**HBA**	**LogP**	**MR (cm^3/mol)**	**TPSA (Å²)[a]**	**LD_{50} (mg/kg)**	**Predicted toxicity[b]**	**HIA (%)**
CUR	368	2	6	3,72	102,80	93,06	2000	4	93,30
BDMC	308	2	4	3,24	89,82	74,60	2560	5	94,20
4	486	1	5	6,51	165,56	85,00	2300	5	92,80

[a]Total polar surface area; [b]Predicted toxicity classification: 1 → 6 (highly toxic to non-toxic).

CUR, DMC, and BDMC all demonstrated pronounced inhibitory efficacy against NO production in macrophages and proliferation of cancer cell lines. Among these, BDMC emerged as a highly promising candidate with potent anti-inflammatory activity through iNOS inhibition mechanisms and selective effects on drug-resistant cancer cell lines. *In silico* studies (molecular docking and molecular dynamics simulations) confirmed and rationalized the structural advantages of BDMC. The absence of flexible methoxy groups enables BDMC to optimize spatial interactions and hydrogen bonding networks, thereby forming thermodynamically more stable complexes with key protein targets such as iNOS and the TLR4/MD-2 complex.

ADMET analysis indicated that curcuminoids, particularly BDMC, possess favorable pharmacokinetic profiles and high safety margins (toxicity classes 4 and 5), reinforcing the basis for their development as potential therapeutic agents.

In vivo validation on animal models of inflammation or cancer is warranted to confirm the therapeutic efficacy and systemic safety of BDMC. Concurrently, molecular biology techniques (Western blot, qPCR, ELISA) should be employed to elucidate the regulatory mechanisms of the NF-κB, STAT3, and iNOS signaling pathways as predicted by computational studies. The docking and MD data obtained herein will serve as an important foundation for the rational design of next-generation BDMC derivatives aimed at optimizing binding affinity, solubility, and bioavailability.

The *in silico* computational simulation approach successfully decoded the mechanisms of action at the molecular level, showing high concordance with *in vitro* results. Specifically, quantum chemical calculations (DFT) elucidated the solvent-dependent antioxidant mechanisms: the aqueous environment favors the single electron transfer (SET) mechanism from anionic species, while the lipid environment favors the proton-coupled electron transfer (PCET) mechanism. Regarding anti-inflammatory activity, molecular docking and molecular dynamics (MD) simulations demonstrated that BDMC and methoxy-deficient derivatives exhibit more stable electrostatic and hydrophobic binding affinities with the target protein complex TLR4/MD-2 compared to CUR.

CONCLUSIONS AND RECOMMENDATIONS

Conclusions

1. Three principal curcuminoid components (CUR, DMC, BDMC) were successfully isolated from *C. longa* rhizomes collected in Vietnam and structurally characterized by modern spectroscopic methods.
2. Three novel hybrid derivatives were synthesized: curcumin-monozerumbone (15% yield), curcumin-biszerumbone (11% yield), and di-propargyl curcumin (21% yield). Structures were confirmed by ^{1}H-NMR, ^{13}C-NMR, and HR-MS.
3. Comprehensive *in vitro* biological evaluation demonstrated that the curcuminoids and their derivatives exhibit antioxidant, anti-inflammatory, cytotoxic, and antimicrobial activities at varying levels.
4. DFT calculations revealed that CUR > BDMC in aqueous environments while BDMC exhibited about 20 fold higher scavenging rate constant than CUR in lipid enviroment. The methoxy group plays an essential role in enhancing the hydrogen-donating capacity of the phenolic hydroxyl group.
5. Docking and MD results demonstrated that curcuminoids are capable of binding to the active site of the TLR4/MD-2 complex, suggesting an anti-inflammatory mechanism through inhibition of the LPS recognition pathway, consistent with the experimental NO inhibition results.
6. The novel nematode species *Scutellonema curcumae* sp. n. parasitizing turmeric in Vietnam was described for the first time, based on morphological and molecular evidence. Nematode infestation significantly reduced curcuminoid content in the rhizomes.

Recommendations

1. Expanding semi-synthesis strategies: Continue the design and synthesis of novel curcuminoid derivatives through new structural modification approaches at the C4 position of the β-diketone system (Knoevenagel condensation) or through transition metal complexation (Zn^{2+}, Cu^{2+}) to optimize solubility and pharmacological properties.
2. Strengthening *in silico* tools: Utilize molecular dynamics (MD) simulation data and pharmacokinetic predictions (ADMET/Lipinski)

as guiding criteria for the rational pre-selection of structural candidates prior to semi-synthesis.

3. Product development applications: The experimental results obtained from purified BDMC and hybrid derivatives provide a robust scientific foundation. It is recommended to pursue further research and development of the following product lines: specialized functional foods with potent antioxidant capacity (BDMC-enriched) targeting lipid environments; anti-inflammatory functional food supplements (BDMC-enriched); semi-synthetic derivatives for cancer treatment support; biological control agents for nematode management; and dermocosmetic applications.